Brain Structure and Function (2019) 224:613–626
https://doi.org/10.1007/s00429-018-1795-x

ORIGINAL ARTICLE

Regulatory roles of perineuronal nets and semaphorin 3A in the postnatal maturation of the central vestibular circuitry for graviceptive reflex

Chun-Wai Ma[1] · Pui-Yi Kwan[1] · Kenneth Lap-Kei Wu[1] · Daisy Kwok-Yan Shum[1,2] · Ying-Shing Chan[1,2]

Received: 19 March 2018 / Accepted: 12 November 2018 / Published online: 20 November 2018

Abstract

Perineuronal nets (PN) restrict neuronal plasticity in the adult brain. We hypothesize that activity-dependent consolidation of PN is required for functional maturation of behavioral circuits. Using the postnatal maturation of brainstem vestibular nucleus (VN) circuits as a model system, we report a neonatal period in which consolidation of central vestibular circuitry for graviception is accompanied by activity-dependent consolidation of chondroitin sulfate (CS)-rich PN around GABAergic neurons in the VN. Postnatal onset of negative geotaxis was used as an indicator for functional maturation of vestibular circuits. Rats display negative geotaxis from postnatal day (P) 9, coinciding with the condensation of CS-rich PN around GABAergic interneurons in the VN. Delaying PN formation, by removal of primordial CS moieties on VN with chondroitinase ABC (ChABC) treatment at P6, postponed emergence of negative geotaxis to P13. Similar postponement was observed following inhibition of GABAergic transmission with bicuculline, in line with the reported role of PN in increasing excitability of parvalbumin neurons. We further reasoned that PN-CS restricts bioavailability of plasticity-inducing factors such as semaphorin 3A (Sema3A) to bring about circuit maturation. Treatment of VN explants with ChABC to liberate PN-bound Sema3A resulted in dendritic growth and arborization, implicating structural plasticity that delays synapse formation. Evidence is thus provided for the role of PN-CS–Sema3A in regulating structural and circuit plasticity at VN interneurons with impacts on the development of graviceptive postural control.

Keywords Perineuronal chondroitin sulfates · Semaphorin 3A · Vestibular system · Development

Introduction

Sensory functions often require experience-dependent fine tuning in a defined period during development to achieve maturation. This period in which development of neural circuits are modulated by sensory input is known as the critical period. In the visual system, consolidation of chondroitin sulfate proteoglycan (CSPG)-rich matrix, known as perineuronal nets (PN), around subsets of GABAergic interneurons in the visual cortex marks the closure of the critical period for ocular dominance plasticity (Hensch 2005; Miyata et al. 2012). PN is a stable structure comprising chondroitin sulfate (CS)-bearing lecticans that are crosslinked by proteins such as tenascin-R or cartilage link protein. Knockout of these protein components prevented PN consolidation resulting in persistent plasticity (Carulli et al. 2010), while disruption of PN-CS with chondroitinase ABC (ChABC) in consolidated PN in the visual cortex reactivated ocular dominance plasticity after the critical period (Pizzorusso et al. 2002, 2006). This implicates key roles of PN-CS proteoglycans in restricting plasticity. Work by others has highlighted the possibility of PN-CS acting as a sponge for the sequestration of soluble extracellular neuronal plasticity-inducing factors such as semaphorin 3A (Sema3A) and

Chun-Wai Ma, Pui-Yi Kwan and Kenneth Lap-Kei Wu contributed equally to this study.

✉ Daisy Kwok-Yan Shum
shumdkhk@hku.hk

✉ Ying-Shing Chan
yschan@hku.hk

[1] School of Biomedical Sciences, Li Ka Shing Faculty of Medicine, The University of Hong Kong, 21 Sassoon Road, Hong Kong SAR, People's Republic of China

[2] State Key Laboratory of Brain and Cognitive Sciences, Li Ka Shing Faculty of Medicine, The University of Hong Kong, 21 Sassoon Road, Hong Kong SAR, People's Republic of China

orthodenticle homeobox 2 (Otx2) (Beurdeley et al. 2012; Dick et al. 2013). In particular, Sema3A was shown to mediate structural plasticity in various brain regions (Morita et al. 2006; Shelly et al. 2011; Uesaka et al. 2014). However, previous work focused on the activation of adult plasticity, leaving the impact of PN-CS in the critical period unclear. Using the postnatal maturation of vestibular system as a model, we asked how consolidation of PN around interneurons in the vestibular nucleus (VN) contributed to the restriction of plasticity that accompanies maturation of the VN circuits.

The VN receives, processes and relays sensory input from the vestibular end organs and proprioceptive afferences. The VN can be further divided into the lateral vestibular nucleus (LV), the superior vestibular nucleus (SuV), the spinal vestibular nucleus (SpV) and the medial vestibular nucleus (MV). The vestibular subnuclei are generated in the order of LV, SuV, SpV and MV between embryonic days 12–14, with the output neurons generated first and the small interneurons generated towards the end (Altman and Bayer 1980). Although vestibular neurons are excitable at birth (Curthoys 1982; Murphy and Du Lac 2001), vestibular reflexes remain immature in the first postnatal week (Wills et al. 2014). This suggests that a critical period for experience-dependent tuning of vestibular circuits extending into the neonatal stage. We used postnatal emergence of negative geotaxis as read-out for maturation of vestibular circuit for gravity detection. Negative geotaxis is the ability for animals to re-orient to a head up position on an inclined plane after being displaced. This is an innate behavior indicative of gravity detection, and can be found in most animals from fruit fly to rat (Kamikouchi et al. 2009; Bouet et al. 2004; Crozier and Pincus 1926). We found vestibular input-dependent consolidation of PN (as indicated by WFA-staining) around GABAergic interneurons of the VN as early as postnatal day (P) 7 in correlation with the acquisition of negative geotaxis. Given involvement of PN in stabilizing synapses and restricting structural plasticity (Orlando et al. 2012; Geissler et al. 2013; Liu et al. 2006), and that the majority of PN enwraps GABAergic interneurons, we hypothesize that retention of plasticity-inducing factor(s) such as Sema3A by PN-CS limits its plasticity at GABAergic neurons in the VN to promote hardwiring of vestibular circuits.

Furthermore, ChABC treatment was reported to increase intracellular chloride ion concentration in hippocampal neurons (Glykys et al. 2014), implicating hyperpolarization. More recently, trimming of PN-CS by ChABC was shown to reduce the firing of parvalbumin-positive neurons in the auditory brainstem of mice (Balmer 2016). We, therefore, reasoned that GABAergic transmission would also play a role in maturation of the VN and found neonatal blockade of GABAergic transmission in the VN with bicuculline to result in similar behavioral deficits as ChABC treatment.

The present study thus revealed three formative processes, namely sensory input, PN establishment around GABAergic interneurons and GABAergic neurotransmission, which are required for the maturation and hardwiring of the central vestibular circuit evidenced by negative geotaxis as a read-out.

Materials and methods

Animals

Sprague Dawley rats, aged P1–21 and young adults (200 g), and adult VGAT-VENUS rats were supplied by the Laboratory Animal Unit, The University of Hong Kong. Animals were allowed free access to food and water and subjected to a 12-h light/dark cycle in an environment maintained at 22 °C. All animal protocols and procedures were performed in accordance to the Guide for the Care and Use of Laboratory Animals (NIH, 2011) and approved by The University of Hong Kong Committee on the Use of Live Animals in Teaching and Research. Table 1 shows the animals used in various experimental groups.

Bilateral Labyrinthectomy (BL)

Animals anesthetized by isoflurane (Abbott, UK) (1.5–2%, 250 cm^3/min) were subjected to BL at P3, P7, P9, or P14. Surgical procedure was performed under a dissecting microscope (Olympus MTX). With a retroauricular approach, the temporalis muscle was dissected to provide access to the bulla. The tympanic membrane and the ear bones were removed. Care was taken to avoid damage to the pterygopalatine artery. The oval window was then opened and enlarged. The endolymph was aspirated and the labyrinth was mechanically ablated. The remaining bony cavity was packed with gelfoam (Ferrosan). The wound was then sutured. The operated rats were allowed to recover under heat from a lamp before they were returned to their dam and reared with their mothers. Postoperative application of lidocaine (Astra) and antibiotic ointment (Furacin; SmithKline Beecham Pharmaceuticals) to the skin wound continued for 3 days. Analgesic (meloxicam, 0.2%) was administered to the mothers via drinking water from 1 day before operation to 1 week post operation. All operated pups showed signs of positive health status. Half of the P3-BL group was sacrificed at P21 and the remaining half was sacrificed at P60 (adult). All other BL groups (P7, P9, P14) were sacrificed at P21. Tissues were prepared for histochemical analysis. Labyrinthine destruction was ascertained by *post-mortem* examination of the temporal bone under a dissecting microscope. The completeness of labyrinthectomy was further

Table 1 Experimental design

A. Histochemical experiments	P3	P5	P7	P9	P11	P12	P13	P14	P21	Adult
WFA[a]										
Normal	–	5	5	5	–	5	–	5	5	5
BL at P3	–	–	–	–	–	–	–	–	5	5
BL at P7 / P9 / P14	–	–	–	–	–	–	–	–	9	–
Saline injection at P6	–	–	–	3	3	–	3	–	3	–
ChABC injection at P6	–	–	–	3	3	–	3	–	3	–
Neurocan										
Normal	5	–	–	–	–	–	–	5	5	5
BL at P3	–	–	–	–	–	–	–	–	5	–
Phosphocan										
Normal	5	–	–	–	–	–	–	5	5	5
WFA + Sema3A	–	–	–	3	–	–	3	–	3	3
WFA + Sema3A (ChABC-treated)	–	–	–	–	–	–	–	–	–	3
WFA + NeuN	–	–	–	–	–	–	–	–	–	3
WFA + Venus + NeuN	–	–	–	–	–	–	–	–	–	3
B. Behavioral experiments (negative geotaxis)										
Normal Control									7 (Tested at P4–P20)	
ChABC at P6									6 (Tested at P7–P20)	
Saline at P6									6 (Tested at P7–P20)	
Bicuculline at P1									10 (Tested at P6–P20)	
C. Analysis of dendritic morphology										
Explant cultures										

[a]Staining for terminal *N*-acetylgalactosamine residues of PN-glycoconjugates

confirmed with use of hematoxylin/ eosin-stained histological sections (8 µm thickness) of the inner ear.

Histochemistry

Rats were sacrificed with overdose of pentobarbital sodium (150 mg/kg, i.p.) and then intracardially perfused with 0.1 M PBS via the ascending aorta, followed by 4% paraformaldehyde (PFA). Brains were postfixed in 4% PFA for 4 h and then cryoprotected in 20% sucrose in 0.2 M PBS overnight at 4 °C. Serial coronal sections (30 µm) of the brainstem containing the vestibular nuclei were prepared on a microtome. Tissue sections were rinsed for 10 min in 0.3% Triton X-100 in 0.1 M PBS, and then processed as free-floating sections before mounting on gelatin-coated slides in DPX (VWR International) or fluorescence mounting medium (Dako).

Lectin staining

Wisteria floribunda agglutinin (biotinylated WFA; Sigma) was used to stain terminal *N*-acetylgalactosamine residues of glycoconjugates in PN. Tissue sections were incubated (4 °C) for 20 h with 1:200 dilution of biotinylated WFA solution in PBS-0.1% BSA, followed by 1 h with avidin–biotin peroxidase complex (1:100 in PBS; Vector). The sections were rinsed in PBS for 3 × 5 min between incubations. Reaction with 0.05% diaminobenzidine (DAB) and 0.005% hydrogen peroxide (H_2O_2) for 5 min at room temperature yielded a brown product. Alternatively, biotinylated WFA staining was visualized with avidin conjugated to FITC (1:200; Vector Lab).

Immunostaining

Non-specific binding sites in sections were blocked off with 0.1 M PBS containing 0.1% BSA, 10% normal goat serum, 0.3% Triton X-100 for 90 min. Sections were then incubated (4 °C) overnight in primary antibody diluted in blocking solution. Primary antibodies included monoclonal anti-neurocan (1:1000, mouse IgG1, Chemicon), monoclonal anti-phosphacan (1:5; mouse IgG1, Developmental Studies Hybridoma Bank), monoclonal anti-neuronal nuclei (NeuN; Chemicon), and polyclonal anti-GABA (1:200; Chemicon). Sections were washed 3 × 5 min with PBS and then incubated with the appropriate secondary antibody diluted in blocking solution for 2 h. The secondary antibodies included biotinylated anti-mouse IgG (1:400; Vector), anti-rabbit IgG

(1:400; Vector), anti-rat IgG (1:400; Vector), Alexa 568-conjugated goat anti-mouse IgG (1:200; Molecular Probes), and Alexa 568-conjugated goat anti-rabbit IgG (1:200; Molecular Probes). Visualization of staining was performed as described in the above paragraph.

Immunocytochemistry

Explant cultures of VN were fixed (in 4% PFA at 37 °C) and incubated (4 °C) overnight in MAP2 antibody (1:200; Sigma) diluted in blocking solution. The cultures were washed 3 × 5 min with PBS and then incubated with the appropriate secondary antibody diluted in blocking solution for 2 h. After washing, the coverslips were mounted on a glass slide with mounting medium with DAPI (Vector Lab).

In all histochemistry or cytochemistry, no non-specific staining was observed on brainstem sections or cultures when WFA or primary antibody was omitted from the protocol. Sections collected from each age-group were processed in parallel. Sections or cultures were examined under a light/fluorescence microscope (Axioplan 2 imaging; Carl Zeiss). Digital images were captured with a CCD camera (Spot; Diagnostic Instrument) connected to a computer. Image preparation, assembly and analysis were performed in Adobe Photoshop 9.0.

Enzyme treatment on tissue sections

Fixed tissue sections were incubated at 37 °C overnight with the bacterial enzyme chondroitinase ABC (*Proteus vulgaris*) (0.1 U/mL; Sigma) in a buffer containing 50 mM Tris (pH 8.0) and 50 mM sodium acetate.

Enzyme injection

Rat pups at P6 were anesthetized by isoflurane (1.5–2%, 250 cm^3/min) and then subjected to bilateral craniotomy (diameter: 2 mm) at sites above the VN (9.1 mm caudal to bregma; 1.5 mm lateral from midline; 3.5 mm beneath the surface of the skull). ChABC (from *Proteus vulgaris*, Sigma, 2 U/mL; 2 µL) or saline (control; 2 µL) was drawn into a pulled borosilicate glass capillary pipette (Harvard Apparatus) and then pressure-injected into each VN using a micromanipulator connected to a PV830 Pneumatic Picopump (World Precision Instruments). The wound was then sutured and the rats were allowed to recover.

Implantation of Elvax slices

Elvax (ethylene–vinyl acetate polymer; Dupont, USA) in dichloromethane was mixed with the $GABA_A$ receptor antagonist bicuculline (Tocris Bioscience) in dimethylsulfoxide to reach 30 mM and then allowed to set at − 80 °C. The desiccated Elvax block was then sectioned into 200 µm-thick slices, 1 mm × 1 mm. Control slices were loaded with saline. The surface of the Elvax slice facing the cerebellar primordium was thinly coated with polycaprolactone (PCL) (Sigma, USA), using a custom-made spraying device (Lai et al. 2016; Wong et al. 2010) to limit diffusion of bicuculline into the cerebellar primordium. In one set of preliminary experiments, Elvax slices loaded with ^{3}H-bicuculline (American Radiolabeled Chemicals, USA) were coated with PCL on both sides. These slices were then immersed in PBS contained in a scintillation vial for a week at 37 °C. Scintillation counting of aliquots of the incubation medium (Schnupp et al. 1995; Smith et al. 1995) revealed only trace amount (~ 5%) of ^{3}H-bicuculline, indicating that PCL coating of the Elvax slice was effective in containing almost all (~ 95%) of the loaded drug within the slice. By contrast, almost all of the ^{3}H-bicuculline loaded into the non-coated Elvax slice was released into the incubation medium.

The skull of P1 rat, anesthetized by isoflurane (1.5–2%, 250 cm^3/min), was opened to expose the obex on the medulla. A piece of bicuculline-loaded Elvax slice was inserted into the IVth ventricle such that the uncoated side of the Elvax slice rested on the surface of the bilateral VN complexes while the PCL-coated side faced the IVth ventricle. During the surgical process, the head of the rat was gently tilted downward such that the space between the brainstem and cerebellar primordium was exposed, allowing the Elvax slice to be inserted horizontally without damaging neural tissue surrounding the IVth ventricle. The skin incision was sutured and the pups were returned to the mother after recovery from anesthesia. These pups showed positive health status, such as daily gain in body weight and stomach full of ingested milk after each meal. These rats were then assessed for postnatal emergence of negative geotaxis. At the end of each experiment, the position of Elvax slice was verified by postmortem examination under a dissecting microscope. In addition, sagittal histological sections of the cerebellum were obtained to confirm that the cerebellum was not damaged. To ensure consistency of treatment across rats, we only included data from rats in which (1) the Elvax slice accurately covered the bilateral VN and (2) the cerebellum was intact.

Negative geotaxis

Negative geotaxis is an innate, counter-gravity response that requires sensory input from the vestibular system (Bouet et al. 2004; Crozier and Pincus 1926; Pincus and Crozier 1929). To ensure that our results would not be affected by visual input, the tests were conducted inside a dark box. An infrared digital camera (Folice Technology) was used to monitor response of the rat following placement in a

nose-down position on a ramp tilted at 45°. Time required to re-orient to nose-up position was recorded. If the time needed was < 20 s, the response was considered as positive. Rats were age-matched (P4–P20) and divided into groups for the test: normal controls, ChABC-injected, saline-injected, or bicuculline-treated. For each group, the percentile achieving the average time required to accomplish negative geotaxis was plotted against age of the rat. The time allowed for the trial was set at an upper limit of 60 s. The trial was terminated if the rat failed to accomplish negative geotaxis response in 60 s.

VN explant culture

Brainstems of P3 rats were harvested. Acute brainstem slices (300 µm) were obtained using a vibratome and then transferred to ice-cold PBS. VN were dissected from the slice under a dissecting microscope and then further cut into 3–4 pieces. The explants were then seeded onto a 12-mm coverslip (Thermo Scientific) or a µ-slide (Ibidi), pre-coated with a mixture of poly-D lysine (50 µg/ml) (SigmaAldrich) and laminin (10 µg/ml) (Life Technology). VN explants were cultured in Neurobasal Medium (ThermoFisher) supplemented with 100x GlutaMAX™ Supplement (ThermoFisher) and B-27 Supplement (50X) (ThermoFisher) at 37 °C, with 5% CO_2. Progenitors migrated from the explant core and formed $MAP2^+$ cells with multiple processes by 15 days in vitro.

Cell counting and statistical analysis

Cell counting was done based on published methods (Lai et al. 2004; Moratalla et al. 1996; Janušonis and Fite 2001). Briefly, in a complete series of coronal brainstem sections, the number of neurons with WFA-stained PN within the confines of each of the anatomically demarcated cell groups of the VN was evaluated under a microscope. Intact PN were defined as those having a distinct and continuous boundary with no breaking point along the outline. The sum of cell counts was divided by the number of tissue sections of that nucleus to yield the mean cell count per section for that nucleus. This computation allows the comparison of cell counts among brainstem nuclei that differ in total cell mass. To confirm reliability of the cell counts, an individual, who was blinded to the experimental paradigm used for each set of brainstem sections, was recruited to repeat the cell counting process of each experiment. Values collected from all counted sections were averaged and data were presented as means ± SEM. Counts in different age-groups were compared using one-way ANOVA followed by Tukey–Kramer multiple comparisons test. Behavioral experiments were analyzed using an unpaired two-tailed Student's *t* test.

For morphological analysis of cultured VN neurons, explant cultures were fixed after 15 days in vitro and stained with MAP2 and DAPI. Flourescent images of individual neurons migrating out from the explant core were acquired using an Olympus microscope. Process length and number, along with number of branches was measured semi-automatically using Metamorph. For each group, 2000–4000 $MAP2^+$ cells were measured. Data were analyzed with one-way ANOVA, and post hoc Turkey's test. In all analyses, a probability value (*P*) of less than 0.05 was taken to be statistically significant.

Results

PN surrounds GABAergic neurons in the VN

WFA-stained PN around the $NeuN^+$ neuronal cell bodies and proximal processes were found in the spinal vestibular nucleus (SpV), medial vestibular nucleus (MV), and lateral vestibular nucleus (LV) of adult rats (Fig. 1a). Use of VGAT-VENUS transgenic rats that expressed VENUS in cells expressing vesicular GABA transporter (VGAT) further showed that PN-bearing neurons in the VN were GABAergic (Fig. 1b).

Postnatal profile of WFA-positive PN in the VN

With postnatal development, progressive intensification and consolidation of WFA-positive PN within the VN was observed as early as P5 in the SpV (Fig. 2a). No neurons in the P1–5 VN showed clear contours of WFA-positive PN. Perineuronal profiles of WFA staining progressed from

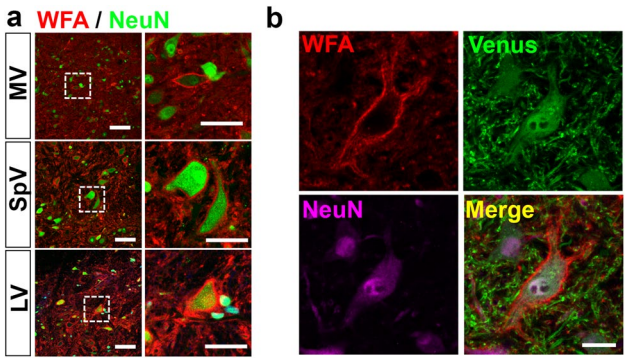

Fig. 1 **a** Photomicrographs showing the morphology of cells with PN in rat LV, SpV and MV. WFA staining (red) was observed at the surface of NeuN-immunopositive neurons (green). Boxed areas enlarged in right panel. **b** NeuN-immunopositive neuron (purple) surrounded by WFA-immunopossitive PN (red) was VGAT-Venus-expressing cell (green). SpV, spinal vestibular nucleus; LV, lateral vestibular nucleus; MV, medial vestibular nucleus. Scale bar, 100 µm for (left panels of **a**); 50 µm for (right panels of **a**); 20 µm for **b**

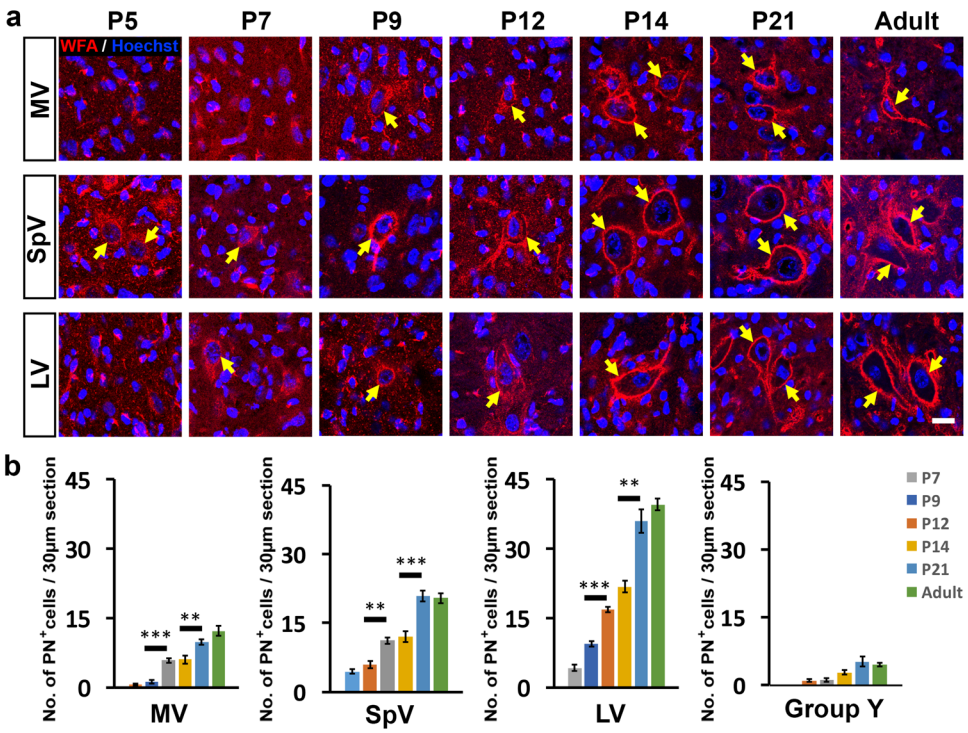

Fig. 2 **a** Photomicrographs showing developmental consolidation of WFA-stained PN (red) in the SpV, MV and LV of rats (P5—adult). In MV, PN (yellow arrows) were observed from P9, while PN in SpV and LV consolidated earlier, at P5 and P7, respectively. Nuclei visualized by Hoechst stain (blue). **b** Histogram showing the number of cells with PN. *$P<0.05$; **$P<0.01$. PN morphology and numver of PN-bearing cells in each VN sub-nucleus was indistinguishable with the adult by P21. SpV, spinal vestibular nucleus; LV, lateral vestibular nucleus; MV, medial vestibular nucleus; y, group y. Scale bar, 100 µm

flocculent and amorphous to solid patches by P3 in the SpV and by P5 in the LV (Fig. 2a). By P7, neurons with consolidated contours of PN were observable in the SpV and LV, but remained somewhat diffuse (Fig. 2a). By P9, PN can be found in the SpV, LV and MV while consolidated PN was observed in the SpV. From P9 onwards, number of PN-bearing cells increased in number in the SpV, LV and MV reaching the adult number by P21 (Fig. 2b; Table 2). The neonatal diffuse pattern of PN was rarely observed at P21; instead, the majority of PN observed was in the adult consolidated form (Fig. 2a). In the SuV, however, only a few neurons with PN were observable (not shown). In group y, PN-bearing neurons were not detectable until P9 and numbers remained low even in the adult (Fig. 2b).

Statistical analysis of the number of PN-bearing neurons in the SpV, MV, and LV revealed significant differences ($P<0.05$) between P9 and P12, P14 and P21, but not beyond P21 (Fig. 2b).

Postnatal profile of neurocan- and phosphacan-positive PN in the VN

Given that WFA only reveals the CS moieties of proteoglycans in PN (Hartig et al. 1994), we pursued the distribution patterns of the core proteins of CS proteoglycans, neurocan and phosphacan, in the SpV and LV (Fig. 3). Similar to WFA-positive PN, both neurocan- and phosphacan-positive PN were barely detectable in the neonate (P3). Progressive

Table 2 Developmental trend of WFA-stained PN in the VN of postnatal and adult rats

Age	P5	P7	P9	P12	P14	P21	Adult
Number of cells with PN							
SpV	0	4.4 ± 0.5***	6.0 ± 0.8***	11.2 ± 0.7***	12.0 ± 1.2***	20.8 ± 1.2	20.4 ± 1.1
MV	0	0.6 ± 0.2***	1.2 ± 0.4***	5.8 ± 0.5***	6.0 ± 0.9**	9.8 ± 0.6	12.2 ± 1.1
LV	0	4.2 ± 0.7***	9.4 ± 0.5***	16.8 ± 0.6***	21.8 ± 1.3***	36.0 ± 2.5	39.6 ± 1.3
Group y	0	0	1.0 ± 0.3***	1.2 ± 0.4***	2.8 ± 0.5*	5.2 ± 1.1	4.6 ± 0.4

Data are presented as mean ± SEM

The number of cells with PN in each vestibular subnucleus was the average of cell counts in each tissue section for that nucleus

The asterisks indicate significant differences (*$P<0.05$; **$P<0.01$; ***$P<0.001$) in the number of cells with PN when compared with the cell counts in adult

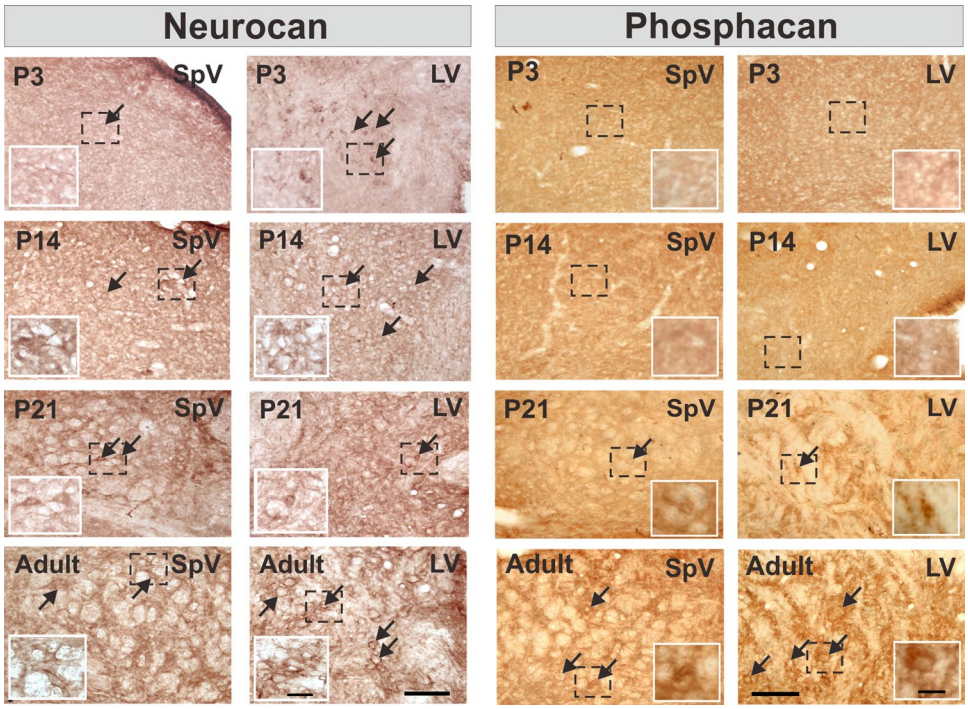

Fig. 3 Photomicrographs showing the expression of neurocan and phosphacan in PN in the SpV and LV of postnatal rats (P3, P14, P21 and adult). Areas bound by the dotted squares are shown at higher magnification in insets. An age-dependent change in the expression of neurocan and phosphacan was observed. SpV, spinal vestibular nucleus; LV, lateral vestibular nucleus. Scale bars, 200 µm; 50 µm for insets

intensification of neurocan- and phophacan-positive PN with age was likewise observed, reaching the adult pattern by P21 (Fig. 3). Whereas the WFA-stained PN changed from diffuse to consolidated with postnatal age, core-protein staining of the PN emerged as condensed features, progressing from patches to perineuronal contours. This suggests that as soon as the proteoglycans were secreted, the core proteins were stably localized to perineuronal binding partners in the perineuronal environment. By contrast, the disposition of CS moieties from diffuse to consolidated suggests that the neonatal forms were not committed to binding partners whereas the postnatal forms may be condensed due to extensive glycan-protein interactions.

Neonatal deprivation of labyrinthine input significantly decreases PN formation in VN

To test if PN formation in the VN is dependent on labyrinth inputs during the formative stage of the central vestibular circuitry, the effects of BL performed at P3 before PN consolidation versus BL at P7, P9 and P14 after PN consolidation had occurred were compared (Fig. 4). All test animals were allowed to survive to adulthood and then sacrificed for the assessment of WFA-stained PN among interneurons in the VN. At P21, no difference in the WFA-stained pattern and the number of PN-bearing cells was observed between normal controls and those which received BL at P7, P9 or P14 (Fig. 4b, d). In contrast, P21 rats which had received BL at P3 showed significantly lower number of PN-bearing neurons (14 ± 1 in the SpV; 6 ± 1 in the MV) than those in corresponding sites of the normal controls (21 ± 1 in the SpV; 10 ± 1 in the MV) ($P < 0.001$) (Fig. 4a, d). Significantly lower number ($P < 0.001$) of PN-bearing cells was observed in the SpV and MV of adult rats (beyond P21) which had received BL at P3 (Fig. 4d) (BL: 14 ± 1 in the SpV and 7 ± 1 in the MV; normal controls: 20 ± 1 in the SpV; 12 ± 1 in the MV). Interestingly, the number of PN-bearing cells in LV was not affected by BL at P3 (Fig. 4a). To find if the changes in WFA-stained PN pattern and number were due to the core protein of CS proteoglycans, some of the experimental and control rats were assessed for neurocan-stained PN in the SpV at P21. Neither the network pattern nor the number of PN-bearing neurons was found to differ between the normal controls and those which received BL at P3 (Fig. 4c). The results, therefore, focused our attention on the PN-CS moieties and their role in vestibular plasticity.

Integrity of PN-CS and GABAergic transmission are required for VN development

Negative geotaxis was used as a behavioral read-out for maturity of the central vestibular circuit for gravity detection. P4–5 rat pups did not re-orient to a nose-up position within 60 s. From P6 onwards, the percentage of rats capable of reaching the nose-up position increased progressively, until 100% at P10 (Fig. 5a). By P9, $\geq 90\%$ of rats displayed negative geotaxis in 20 s. From P12 onwards, only ~ 5 s was needed and such performance was consistent thereafter. We, therefore, adopted 20 s as the threshold time for the completion of negative geotaxis as indication of near-maturity in the

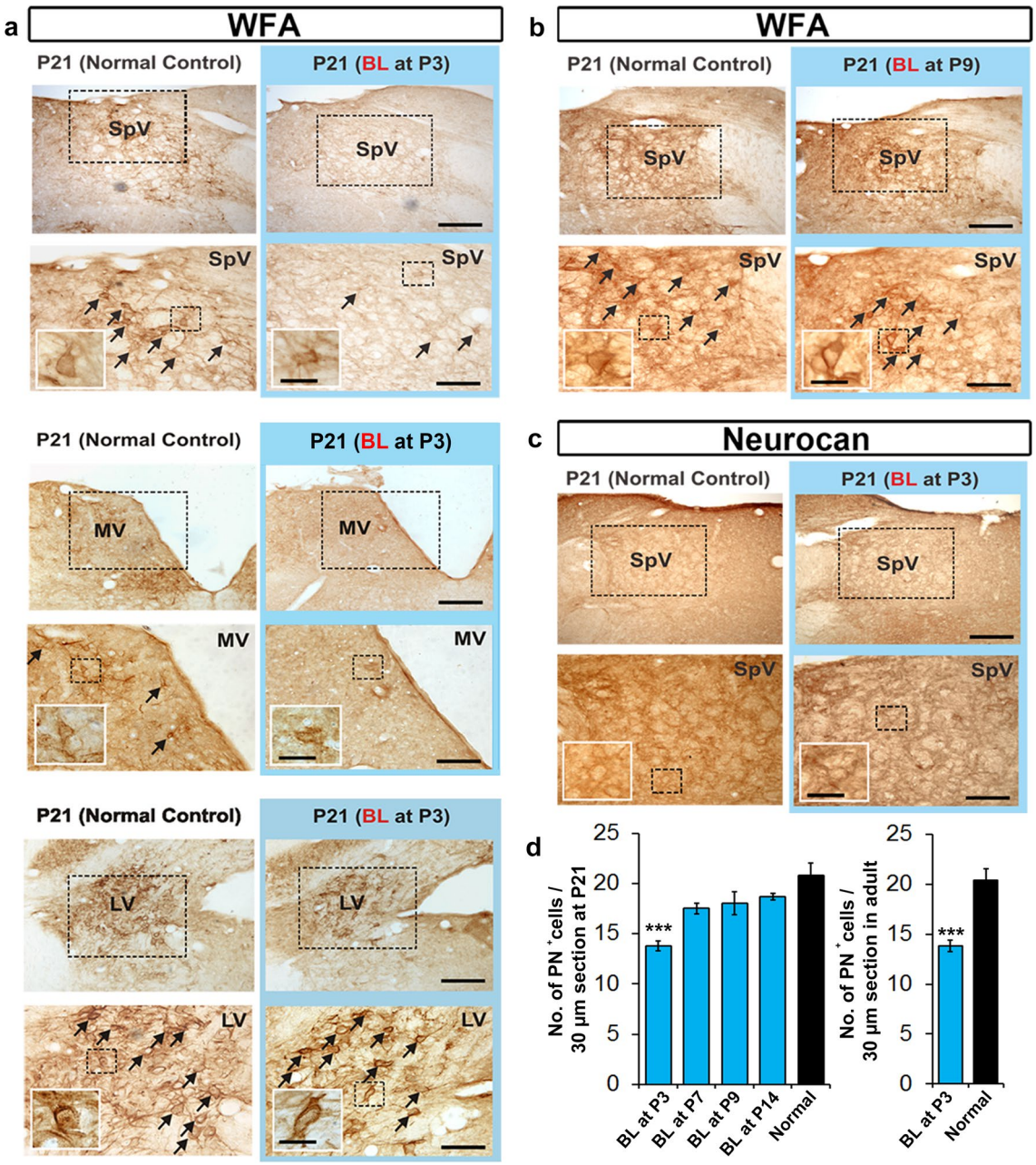

Fig. 4 Difference in the expression pattern of WFA-stained PN in the SpV, MV and LV was observed at P21 between normal rats and rats which received bilateral labyrinthectomy (BL) at P3 (**a**), but not at P9 (**b**). For the rats which received BL at P3 (but not at P7, P9 and P14) and were allowed to survive until P21, the number of cells surrounded by PN was significantly lower than those in corresponding sites of the normal controls (**d**). No difference in the expression pattern of neurocan-based PN in the VN was observed between normal P21 rats and those which received BL at P3 (**c**). Areas bound by the dotted squares are shown at higher magnification in insets. The asterisk indicates significant difference (***$P<0.001$) in cell count between two groups. Arrow: cells with PN. SpV, spinal vestibular nucleus. Scale bars, 400 µm (upper panels) and 200 µm (lower panels) for **a–c**; 50 µm for insets

central vestibular circuitry. Neonatal deprivation of labyrinthine inputs by BL completely abolished negative geotaxis behavior with no recovery even at the adult stage, indicating that it is vestibular-dependent and that proprioceptive input alone cannot support negative geotaxis.

We then attempted to perturb PN-CS and CS-dependent binding of ligands by injection of ChABC into the VN of rats at P6 when PN-CS was detectable but not yet consolidated. Rats that had been injected with ChABC showed delay in the acquisition of negative geotaxis, from P9 (normal controls) to P13 (ChABC-treated) (Fig. 5a).

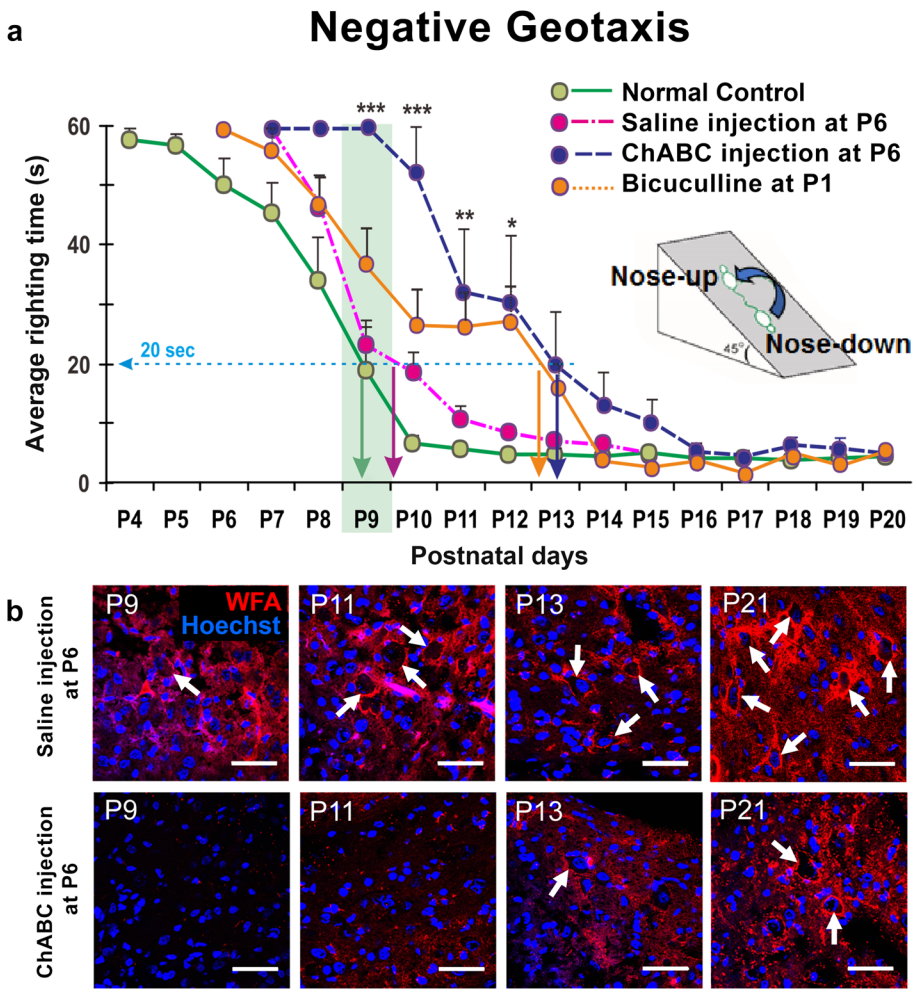

Fig. 5 PN formation correlates with maturation of vestibular function. **a** Normal rats acquired the mature response at P9 (when PN started to consolidate), but the acquisition of negative geotaxis was delayed to P13 in rats pretreated with chondroitinase ABC (ChABC) at P6 or bicuculline at P1. $*P<0.05$; $**P<0.01$; $***P<0.001$ indicate significant differences between normal and ChABC-treated groups in the time taken to accomplish the response. Cartoon illustrates the negative geotaxis response. **b** WFA-positive PN is consolidated in saline-injected rats by P9. Injection of ChABC into the MV at P6 delayed consolidation of WFA-positive PN (red) to P13 (white arrows), co-incident with maturation of negative geotaxis behavior. Nuclei were visualized by Hoechst stain (blue). Arrows point to cells with PN. Scale bar: 50 µm

Before P10, none of the ChABC-treated rats displayed negative geotaxis in 20 s. From P10 onwards, the percentage of ChABC-treated rats capable of reaching the nose-up position within 20 s increased progressively, reaching ≥ 80% by P13 and 100% by P15. After injection on P6, WFA-stained PN were found in the MV from P9 in saline control but were barely discernible in ChABC-treated rats (Fig. 5b). Notably, negative geotaxis behavior matured in ChABC-treated rats when PN was first discernible at P13, suggesting close correlation between PN consolidation and behavioral maturation.

The vast majority of PN-bearing neurons in the VN are GABAergic neurons. Since loss of PN-CS was reported to reduce excitability and spiking rate of inhibitory neurons (Balmer 2016), we asked whether delayed emergence of negative geotaxis could result from inadequate GABAergic transmission at GABAergic interneurons in the VN. To address this, Elvax loaded with $GABA_A$ receptor antagonist bicuculline was implanted onto the VN of rat pups at P1 to block GABAergic transmission. Rats were then monitored for display of negative geotaxis along the postnatal time course up to P20. Similar to perturbation of PN-CS, antagonizing GABAergic transmission in the VN brought about a delay in the acquisition of negative geotaxis, from P9 (normal controls) to P13 (bicuculline-treated) (Fig. 5a).

Increased localization of Sema3A to PN in the VN during Postnatal Development

Given that Sema3A is a plasticity-inducing factor with binding affinity for PN-CS in the adult brain extract (Dick et al. 2013), we asked whether sequestration of Sema3A by PN restricted its access to the neuronal cell surface to limit plasticity. Double fluorescence staining for WFA and Sema3A found Sema3A in colocalization with PN (Fig. 6a). The extent of colocalization varied with the VN subnuclei but invariably increased with postnatal age (Fig. 6a). The SpV and MV showed trends of low-to-moderate colocalization in P9-13 tissues, reaching maximal colocalization

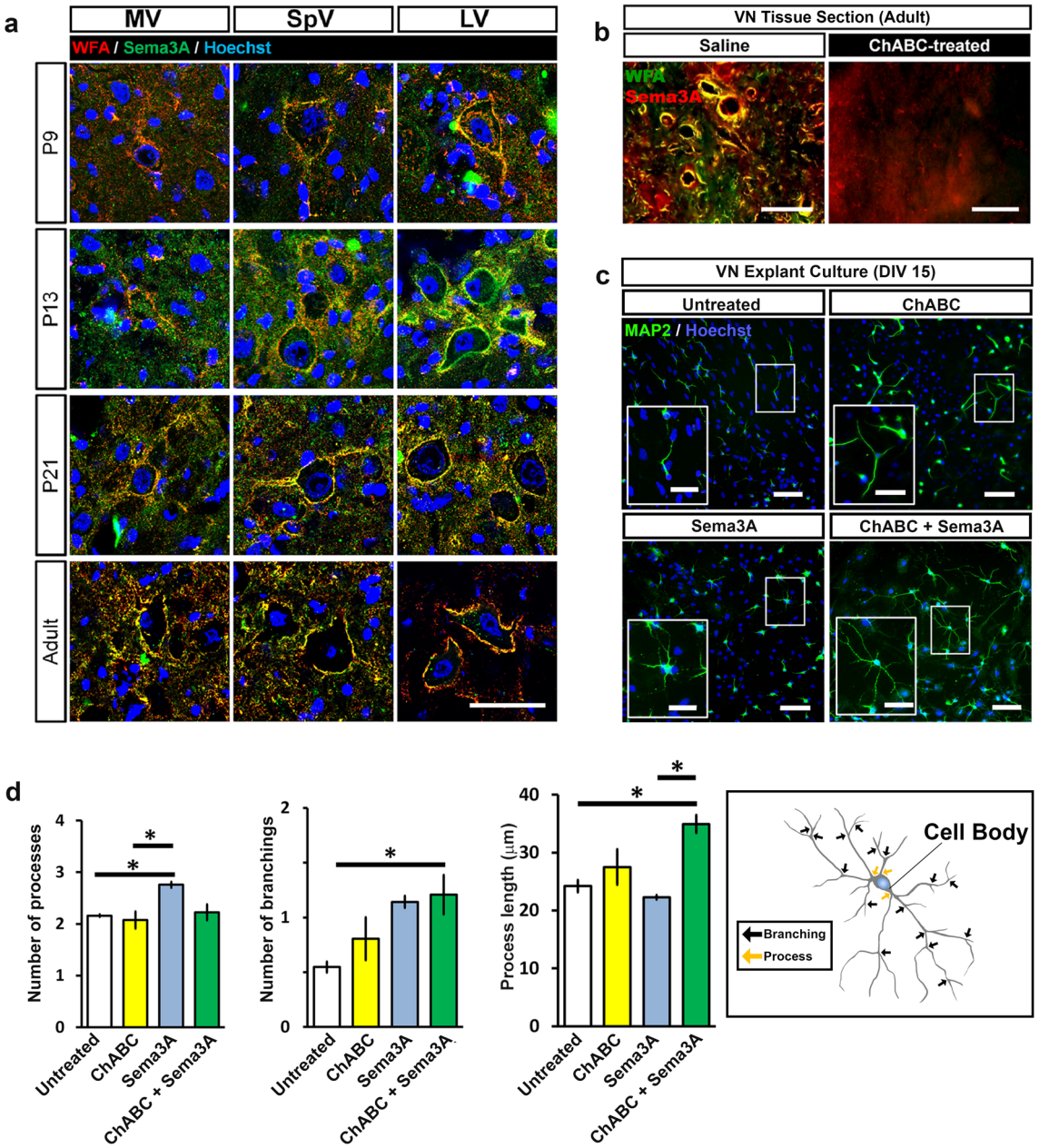

Fig. 6 **a** Colocalization of WFA-stained PN (red) and Sema3A (green) in the VN during postnatal development. **b** In adult VN tissue sections, removal of CS with ChABC treatment resulted in a loss of Sema3A signals. **c** ChABC and Sema3A treatment increased branching and process length of DIV 15 cultured VN neurons (indicated by MAP2 immunoreactivity (green) and Hoechst-stained nuclei (blue)). **d** Morphological analysis of neurons in VN explant culture (DIV 15) after treatment with ChABC, Sema3A or co-treatment with ChABC and Sema3A. Schematic diagram illustrates definition of processes (yellow arrows), primary extensions from the cell body; and branching (black arrows). Number of processes, number of branchings and process length were analyzed. Co-treatment of ChABC and Sema3A significantly enhanced the growth and arborization of neurites. Neither Sema3A nor ChABC alone significantly enhanced the length of processes. $*p<0.05$, $**p<0.01$. *SpV* spinal vestibular nucleus; *LV* lateral vestibular nucleus; *MV* medial vestibular nucleus. Scale bars, 100 μm for **(a)** and **(b)**; 200μ m for **(c)** and 50 μm for insets in **c**

in the P21 and adult tissues. In the LV, colocalization was low in P9 tissue, reached maximal in P13- 21 tissues and thereafter, Sema3A abundance apparently subsided whereas WFA-stained PN remained. The results suggested that affinity of PN-CS for Sema3A differed with the VN subnuclei and with postnatal age. Digestion of PN-CS with ChABC treatment in VN tissue sections resulted in a loss of Sema3A signals, indicating that Sema3A was associated with PN-CS and subsequently became diffusible with the digestion of CS (Fig. 6b).

To demonstrate that CS restricts the potency of Sema3A, cultured VN neurons were treated with either ChABC, Sema3A or a combination of both (Fig. 6c). It can be seen that Sema3A increases dendritic branching and growth of VN neurons (Fig. 6d). The effect of Sema3A became more pronounced after treatment with ChABC to remove CS from the perineuronal matrix, demonstrating that perineuronal CS limits interaction between Sema3A and its receptors. "Number of processes" was not significantly changed after ChABC treatment (Fig. 6d). This suggested that the consequence of Sema3A action is revealed at the axonal and dendritic growth cones but not at the sites of primary outgrowth from the neuronal soma.

Discussion

Closure of formative periods for the development of sensorimotor circuits are often accompanied by consolidation of PN around GABAergic interneurons in the circuit (Balmer et al. 2009; Hensch 2005; Nabel and Morishita 2013). Here, we report that postnatal emergence of negative geotaxis in rats is subject to a formative period in the graviceptive circuit of the VN. During this period, sensory input, consolidation of PN-CS, and GABAergic neurotransmission in the VN circuit are required for circuit maturation. Perturbation of any one of these components affected the emergence of negative geotaxis. The plasticity factor Sema3A was shown to be increasingly retained by PN-CS during development, suggesting a restriction of Sema3A bioavailability by PN-CS. Removal of such plasticity-inducing factors thus stabilizes inhibitory interneurons in the VN for hardwiring the circuit for negative geotaxis.

WFA-positive PN presentation in the neonatal VN

We demonstrate that the CS-moieties of PN, as denoted by WFA-positivity at GABAergic interneurons in the VN change progressively from flocculent and amorphous presentations in the neonate to consolidated patches and contours in postnatal stages up to adulthood (Fig. 2). This is distinct from consolidation profiles of the core proteins of PN chondroitin sulfate proteoglycans, neurocan and phosphacan (Bandtlow and Zimmermann 2000; Jones et al. 2003), which appeared as dense patches that linked together to form the net with age (Fig. 3). Core proteins of other PN components, such as aggrecan, brevican, versican, and tenascin-R, were shown to consolidate similarly (Carulli et al. 2006). This suggests that the core proteins are clustered upon secretion to the perineuronal environment, while their CS moieties are not yet condensed due either to lack of CS-binding molecules in the early neonatal environment or low affinity of neonatal CS moieties for such molecules.

Activity-dependent formation of PN in the VN during development

In the present study, sensory deprivation of the vestibular system induced by neonatal BL decreased PN formation. This is in line with studies in other sensory systems where sensory deprivation also delayed consolidation of PN, such as animals treated with visual deprivation induced by dark rearing (Pizzorusso et al. 2002) and somatosensory deprivation by whisker trimming (McRae et al. 2007) at a neonatal stage. Following BL in neonatal rats, the pattern of PN and the number of VN neurons with PN were frozen at the neonatal state (Fig. 4a, d), resulting in a permanent reduction of PN in the VN compared to sham control adults. Given that BL rats do not display negative geotaxis or other graviceptive behavior, it is likely that reduction in PN results in long-term change in the processing of vestibular information. Interestingly, the LV, which is known to receive dense spinovestibular input from the limb (Matsuyama and Drew 2000; Marlinsky 1992), did not show significant decrease of PN after BL at P3 (Fig. 4a). However, unlike postural maintenance which could be supported by proprioceptive cues alone (Deliagina and Orlovsky 2002), negative geotaxis never emerged in animals with BL. This is consistent with observations in other mammals after BL (Dow 1938).

Critical period for PN formation in the VN

The number of WFA-stained PN reached adult level at P21 in normal rats (Fig. 2b). However, for rats which received BL at P3 (i.e. at a time before PN consolidation around VN neurons), the number of VN neurons with PN at P21 was ~ 30% lower than those of the normal controls (Fig. 4d). In contrast, no significant difference in the number of VN neurons with PN was observed between normal P21 rats and those which received BL at P7, P9 or P14 (Fig. 4d). This suggests a time window for the initiation of PN formation between P3–7. Once the process of PN formation has been initiated, activity from the vestibular afferents is no longer critical to the maintenance of PN into adulthood. Whether this is generally true throughout the brain remains to be proven.

Roles of WFA-stained PN on maturation of vestibular behavior

We observed maturation of negative geotaxis at P9 (Fig. 5a), coincident with PN consolidation (Fig. 5b). Interestingly, by delaying PN consolidation to P13 with ChABC injection into the VN at P6, we were able to delay emergence of negative geotaxis accordingly (Fig. 5b). Inflammatory processes or microglia activation in the brain after surgical lesion has been shown to mediate synaptic stripping (Cullheim and

Thams 2007; Chirumamilla et al. 2002). To assess the effect of surgical lesion on delayed maturation of circuits, surgical controls for invasive procedures, i.e. saline injection as control for ChABC injection, PBS-loaded Elvax slice as control for bicuculline-loaded Elvax slice, and sham operation for BL, have been included. It was found that behavioral performance of saline control animals did not differ from wild type (Fig. 5a), suggesting that these processes did not contribute significantly to the observed delay in the maturation of VN circuits. Furthermore, we previously characterized maturation of VN circuits for otolith and canal input, and found that functional connectivity between the vestibular end organs and central VN neurons was formed 1 week after birth (Ma et al. 2013; Lai and Chan 2001; Lai et al. 2006, 2004). This coincided with initiation of PN consolidation in the VN (Fig. 2; Table 2). VN neurons responsive to vestibular stimulation became dramatically more abundant at P14 as PN became more consolidated and levelled off as PN reached the adult level at P21. These suggest that PN is required for stabilization of synapses resulting in maturation of functional circuits.

Since PN in the VN primarily surrounds GABAergic neurons (Fig. 1b), we reasoned that cleavage of CS moieties of PN with ChABC likely influenced vestibular behavior by modulating GABAergic transmission in the VN. We showed that the acquisition of vestibular behavior was also delayed to P13 in rats pretreated with $GABA_A$ receptor antagonist at P1 (Fig. 5a), suggesting that GABAergic transmission plays a key role for the maturation of negative geotaxis. Indeed, GABAergic transmission in the VN has been shown to play crucial roles in vestibular function (Buttner et al. 1992; Dieterich et al. 1991; Gliddon et al. 2005; Kato et al. 2003; Nakamura et al. 1989; Reber et al. 1996; Tighilet and Lacour 2001).While it has been shown that GABAergic neurons in the cortex with PN have increased firing rates (Balmer 2016), more experiments will be required to demonstrate that this is the case in the VN. Nonetheless, our results highlight GABAergic transmission in the critical period as one of the keys for consolidation of vestibular circuits.

Role of Sema3A on maturation of vestibular behavior

In addition to direct modulation of the intrinsic properties of the neuron, sequestration of plasticity factors by PN-CS may also work to limit structural plasticity. One such factor, Sema3A, was reported to interact with CS type E of the PN (Dick et al. 2013). Indeed, we found colocalization of Sema3A to PN-CS in the VN (Fig. 6a, b). Sema3A induces structural plasticity of cortical (Morita et al. 2006) and hippocampal (Shelly et al. 2011) neurons in culture as well as cerebellar neurons in vivo (Carulli et al. 2013; Uesaka et al. 2014). When applied to cultured VN neurons, Sema3A increased growth and branching of neuronal processes (Fig. 6c, d). Removal of perineuronal CS with ChABC further enhanced the plasticity-inducing effects of Sema3A (Fig. 6c, d). This supports the idea that PN-CS limits the bioavailability/ plasticity-inducing properties of Sema3A, thereby limiting aberrant structural plasticity that delays synapse formation, and as a consequence promotes the hardwiring of the central pathway for vestibular behavior.

Concluding remarks

Taken together, our results indicate that (1) sensory input within the first postnatal week initiates PN formation; (2) PN consolidation is linked with functional maturation of vestibular circuits; (3) inhibition of GABAergic transmission within the VN resulted in similar behavioral deficits as enzymatic degradation of PN-CS; (4) PN-CS limits the potency of plasticity-inducing factors such as Sema3A to bring about decrease in structural plasticity required for hardwiring of circuits. This study establishes the key processes required in the first postnatal week for the maturation of VN circuits for the emergence of graviceptive negative geotaxis behavior. While it is likely that such processes are inter-linked, further investigation is required to establish a definite causal relationship. The study further provides insight into PN components that can be targeted to modulate neural plasticity for regeneration or recovery from neurological disorders. Identification of plasticity-inducing factors that are modulated via their interaction with PN would greatly benefit our understanding of how PN mediates such a plethora of vital functions.

Acknowledgements The authors are grateful to Simon S.M. Chan, Kimmy F.L. Tsang and Alice Y.Y. Lui of The University of Hong Kong for their excellent assistance in the experiments.

Funding This work was supported by grants of the Hong Kong Research Grants Council (RGC HKU77681212, 17125115, N_HKU735/14).

Compliance with ethical standards

Conflict of interest The authors declare that they have no conflict of interest.

Ethical approval All applicable international, national, and/or institutional guidelines for the care and use of animals were followed. All procedures performed in studies involving animals were in accordance with the ethical standard of the institution of practice at which the studies were conducted. All animal protocols and procedures were performed in accordance to the Guide for the Care and Use of Laboratory Animals (NIH, 2011) and approved by The University of Hong Kong Committee on the Use of Live Animals in Teaching and Research. This article does not contain any human participants performed by any of the authors.

References

Altman J, Bayer SA (1980) Development of the brain stem in the rat. III. Thymidine-radiographic study of the time of origin of neurons of the vestibular and auditory nuclei of the upper medulla. J Comp Neurol 194(4):877–904

Balmer TS (2016) Perineuronal nets enhance the excitability of fast-spiking neurons. eNeuro 3(4):0112–0116

Balmer TS, Carels VM, Frisch JL, Nick TA (2009) Modulation of perineuronal nets and parvalbumin with developmental song learning. J Neurosci 29(41):12878–12885. https://doi.org/10.1523/JNEUROSCI.2974-09.2009

Bandtlow CE, Zimmermann DR (2000) Proteoglycans in the developing brain: new conceptual insights for old proteins. Physiol Rev 80(4):1267–1290

Beurdeley M, Spatazza J, Lee HH, Sugiyama S, Bernard C, Di Nardo AA, Hensch TK, Prochiantz A (2012) Otx2 binding to perineuronal nets persistently regulates plasticity in the mature visual cortex. J Neurosci 32(27):9429–9437

Bouet V, Wubbels RJ, de Jong HA, Gramsbergen A (2004) Behavioural consequences of hypergravity in developing rats. Brain Res Dev Brain Res 153(1):69–78. https://doi.org/10.1016/j.devbrainres.2004.03.022

Buttner U, Straube A, Kurzan R (1992) Oculomotor effects of gamma-aminobutyric acid agonists and antagonists in the vestibular nuclei of the alert monkey. Ann N Y Acad Sci 656:645–659

Carulli D, Rhodes KE, Brown DJ, Bonnert TP, Pollack SJ, Oliver K, Strata P, Fawcett JW (2006) Composition of perineuronal nets in the adult rat cerebellum and the cellular origin of their components. J Comp Neurol 494(4):559–577. https://doi.org/10.1002/cne.20822

Carulli D, Pizzorusso T, Kwok JC, Putignano E, Poli A, Forostyak S, Andrews MR, Deepa SS, Glant TT, Fawcett JW (2010) Animals lacking link protein have attenuated perineuronal nets and persistent plasticity. Brain 133(8):2331–2347

Carulli D, Foscarin S, Faralli A, Pajaj E, Rossi F (2013) Modulation of semaphorin3A in perineuronal nets during structural plasticity in the adult cerebellum. Mol Cell Neurosci 57:10–22. https://doi.org/10.1016/j.mcn.2013.08.003

Chirumamilla S, Sun D, Bullock M, Colello R (2002) Traumatic brain injury induced cell proliferation in the adult mammalian central nervous system. J Neurotrauma 19(6):693–703

Crozier WJ, Pincus G (1926) Tropisms of Mammals. Proc Natl Acad Sci USA 12(10):612–616

Cullheim S, Thams S (2007) The microglial networks of the brain and their role in neuronal network plasticity after lesion. Brain Res Rev 55(1):89–96

Curthoys I (1982) Postnatal developmental changes in the response of rat primary horizontal semicircular canal neurons to sinusoidal angular accelerations. Exp Brain Res 47(2):295–300

Deliagina TG, Orlovsky GN (2002) Comparative neurobiology of postural control. Curr Opin Neurobiol 12(6):652–657

Dick G, Tan CL, Alves JN, Ehlert EM, Miller GM, Hsieh-Wilson LC, Sugahara K, Oosterhof A, van Kuppevelt TH, Verhaagen J (2013) Semaphorin 3A binds to the perineuronal nets via chondroitin sulfate type E motifs in rodent brains. J Biol Chem 288(38):27384–27395

Dieterich M, Straube A, Brandt T, Paulus W, Buttner U (1991) The effects of baclofen and cholinergic drugs on upbeat and downbeat nystagmus. J Neurol Neurosurg Psychiatry 54(7):627–632

Dow RS (1938) The effects of unilateral and bilateral labyrinthectomy in monkey, baboon and chimpanzee. Am J Physiol Legacy Content 121(2):392–399

Geissler M, Gottschling C, Aguado A, Rauch U, Wetzel CH, Hatt H, Faissner A (2013) Primary hippocampal neurons, which lack four crucial extracellular matrix molecules, display abnormalities of synaptic structure and function and severe deficits in perineuronal net formation. J Neurosci 33(18):7742–7755. https://doi.org/10.1523/JNEUROSCI.3275-12.2013

Gliddon CM, Darlington CL, Smith PF (2005) GABAergic systems in the vestibular nucleus and their contribution to vestibular compensation. Prog Neurobiol 75(1):53–81. https://doi.org/10.1016/j.pneurobio.2004.11.001

Glykys J, Dzhala V, Egawa K, Balena T, Saponjian Y, Kuchibhotla KV, Bacskai BJ, Kahle KT, Zeuthen T, Staley KJ (2014) Local impermeant anions establish the neuronal chloride concentration. Science 343(6171):670–675. https://doi.org/10.1126/science.1245423

Hartig W, Brauer K, Bigl V, Bruckner G (1994) Chondroitin sulfate proteoglycan-immunoreactivity of lectin-labeled perineuronal nets around parvalbumin-containing neurons. Brain Res 635(1–2):307–311

Hensch TK (2005) Critical period plasticity in local cortical circuits. Nat Rev Neurosci 6(11):877–888. https://doi.org/10.1038/nrn1787

Janušonis S, Fite KV (2001) Diurnal variation of c-Fos expression in subdivisions of the dorsal raphe nucleus of the Mongolian gerbil (*Meriones unguiculatus*). J Comp Neurol 440(1):31–42

Jones LL, Margolis RU, Tuszynski MH (2003) The chondroitin sulfate proteoglycans neurocan, brevican, phosphacan, and versican are differentially regulated following spinal cord injury. Exp Neurol 182(2):399–411

Kamikouchi A, Inagaki HK, Effertz T, Hendrich O, Fiala A, Gopfert MC, Ito K (2009) The neural basis of Drosophila gravity-sensing and hearing. Nature 458(7235):165–171. https://doi.org/10.1038/nature07810

Kato R, Iwamoto Y, Yoshida K (2003) Contribution of GABAergic inhibition to the responses of secondary vestibular neurons to head rotation in the rat. Neurosci Res 46(4):499–508

Lai CH, Chan YS (2001) Spontaneous discharge and response characteristics of central otolith neurons of rats during postnatal development. Neuroscience 103(1):275–288

Lai CH, Tse YC, Shum DK, Yung KK, Chan YS (2004) Fos expression in otolith-related brainstem neurons of postnatal rats following off-vertical axis rotation. J Comp Neurol 470(3):282–296. https://doi.org/10.1002/cne.11048

Lai SK, Lai CH, Yung KK, Shum DK, Chan YS (2006) Maturation of otolith-related brainstem neurons in the detection of vertical linear acceleration in rats. Eur J Neurosci 23(9):2431–2446. https://doi.org/10.1111/j.1460-9568.2006.04762.x

Lai CH, Ma CW, Lai SK, Han L, Wong HM, Yeung KW, Shum DK, Chan YS (2016) Maturation of glutamatergic transmission in the vestibulo-olivary pathway impacts on the registration of head rotational signals in the brainstem of rats. Brain Struct Funct 221(1):217–238. https://doi.org/10.1007/s00429-014-0903-9

Liu J, Chau CH, Liu H, Jang BR, Li X, Chan YS, Shum DK (2006) Upregulation of chondroitin 6-sulphotransferase-1 facilitates Schwann cell migration during axonal growth. J Cell Sci 119(Pt 5):933–942. https://doi.org/10.1242/jcs.02796

Ma CW, Zhang FX, Lai CH, Lai SK, Yung KK, Shum DK, Chan YS (2013) Postnatal expression of TrkB receptor in rat vestibular nuclear neurons responsive to horizontal and vertical linear accelerations. J Comp Neurol 521(3):612–625. https://doi.org/10.1002/cne.23193

Marlinsky V (1992) Activity of lateral vestibular nucleus neurons during locomotion in the decerebrate guinea pig. Exp Brain Res 90(3):583–588

Matsuyama K, Drew T (2000) Vestibulospinal and reticulospinal neuronal activity during locomotion in the intact cat. I. Walking on a level surface. J Neurophysiol 84(5):2237–2256. https://doi.org/10.1152/jn.2000.84.5.2237

McRae PA, Rocco MM, Kelly G, Brumberg JC, Matthews RT (2007) Sensory deprivation alters aggrecan and perineuronal net expression in the mouse barrel cortex. J Neurosci 27(20):5405–5413. https://doi.org/10.1523/JNEUROSCI.5425-06.2007

Miyata S, Komatsu Y, Yoshimura Y, Taya C, Kitagawa H (2012) Persistent cortical plasticity by upregulation of chondroitin 6-sulfation. Nat Neurosci 15(3):414–422. https://doi.org/10.1038/nn.3023 **(S411–412)**

Moratalla R, Elibol B, Vallejo M, Graybiel AM (1996) Network-level changes in expression of inducible Fos–Jun proteins in the striatum during chronic cocaine treatment and withdrawal. Neuron 17(1):147–156

Morita A, Yamashita N, Sasaki Y, Uchida Y, Nakajima O, Nakamura F, Yagi T, Taniguchi M, Usui H, Katoh-Semba R, Takei K, Goshima Y (2006) Regulation of dendritic branching and spine maturation by semaphorin3A-Fyn signaling. J Neurosci 26(11):2971–2980. https://doi.org/10.1523/JNEUROSCI.5453-05.2006

Murphy GJ, Du Lac S (2001) Postnatal development of spike generation in rat medial vestibular nucleus neurons. J Neurophysiol 85(5):1899–1906

Nabel EM, Morishita H (2013) Regulating critical period plasticity: insight from the visual system to fear circuitry for therapeutic interventions. Front Psychiatry 4:146. https://doi.org/10.3389/fpsyt.2013.00146

Nakamura J, Sasa M, Takaori S (1989) Ethanol potentiates the effect of gamma-aminobutyric acid on medial vestibular nucleus neurons responding to horizontal rotation. Life Sci 45(11):971–978

Orlando C, Ster J, Gerber U, Fawcett JW, Raineteau O (2012) Perisynaptic chondroitin sulfate proteoglycans restrict structural plasticity in an integrin-dependent manner. J Neurosci 32(50):18009–18017. https://doi.org/10.1523/JNEUROSCI.2406-12.2012

Pincus G, Crozier WJ (1929) On the geotropic response in young rats. Proc Natl Acad Sci USA 15(7):581–586

Pizzorusso T, Medini P, Berardi N, Chierzi S, Fawcett JW, Maffei L (2002) Reactivation of ocular dominance plasticity in the adult visual cortex. Science 298(5596):1248–1251. https://doi.org/10.1126/science.1072699

Pizzorusso T, Medini P, Landi S, Baldini S, Berardi N, Maffei L (2006) Structural and functional recovery from early monocular deprivation in adult rats. Proc Natl Acad Sci USA 103(22):8517–8522. https://doi.org/10.1073/pnas.0602657103

Reber A, Poitevin B, Leroy MH, Nzobounsana V (1996) Optokinetic and vestibulo-ocular reflex adjustment by GABA antagonists. Behav Brain Res 81(1–2):89–97

Schnupp JW, King AJ, Smith AL, Thompson ID (1995) NMDA-receptor antagonists disrupt the formation of the auditory space map in the mammalian superior colliculus. J Neurosci 15(2):1516–1531

Shelly M, Cancedda L, Lim BK, Popescu AT, Cheng PL, Gao H, Poo MM (2011) Semaphorin3A regulates neuronal polarization by suppressing axon formation and promoting dendrite growth. Neuron 71(3):433–446. https://doi.org/10.1016/j.neuron.2011.06.041

Smith AL, Cordery PM, Thompson ID (1995) Manufacture and release characteristics of Elvax polymers containing glutamate receptor antagonists. J Neurosci Methods 60(1–2):211–217

Tighilet B, Lacour M (2001) Gamma amino butyric acid (GABA) immunoreactivity in the vestibular nuclei of normal and unilateral vestibular neurectomized cats. Eur J Neurosci 13(12):2255–2267

Uesaka N, Uchigashima M, Mikuni T, Nakazawa T, Nakao H, Hirai H, Aiba A, Watanabe M, Kano M (2014) Retrograde semaphorin signaling regulates synapse elimination in the developing mouse brain. Science 344(6187):1020–1023. https://doi.org/10.1126/science.1252514

Wills TJ, Muessig L, Cacucci F (2014) The development of spatial behaviour and the hippocampal neural representation of space. Phil Trans R Soc B 369(1635):20130409

Wong HM, Yeung KW, Lam KO, Tam V, Chu PK, Luk KD, Cheung KM (2010) A biodegradable polymer-based coating to control the performance of magnesium alloy orthopaedic implants. Biomaterials 31(8):2084–2096. https://doi.org/10.1016/j.biomaterials.2009.11.111